Water Research 148 (2019) 398–406

Contents lists available at ScienceDirect

Water Research

journal homepage: www.elsevier.com/locate/watres

Response of chloramphenicol-reducing biocathode resistome to continuous electrical stimulation

Bin Liang [a, b], Jincai Ma [c], Weiwei Cai [d, b], Zhiling Li [b], Wenzong Liu [a], Mengyuan Qi [b], Youkang Zhao [b], Xiaodan Ma [b], Ye Deng [a], Aijie Wang [a, b, *], Jizhong Zhou [e]

[a] Key Laboratory of Environmental Biotechnology, Research Center for Eco-Environmental Sciences, Chinese Academy of Sciences, Beijing, 100085, China
[b] State Key Laboratory of Urban Water Resource and Environment, Harbin Institute of Technology, Harbin, 150090, China
[c] College of Environment and Resources, Jilin University, Changchun, 130021, China
[d] School of Civil Engineering, Beijing Jiaotong University, Beijing, 100044, China
[e] Institute for Environmental Genomics and Department of Microbiology and Plant Biology, University of Oklahoma, Norman, OK, 73019, USA

ARTICLE INFO

Article history:
Received 18 July 2018
Received in revised form
21 October 2018
Accepted 25 October 2018
Available online 30 October 2018

Keywords:
Chloramphenicol (CAP) reduction
Biocathode resistome
Continuous electrical stimulation
Antibiotic resistance genes (ARGs)
Network complexity

ABSTRACT

Understanding the fate of overall antibiotic resistance genes (ARGs) during the biological treatment of antibiotic containing wastewater is a central issue for the water ecological safety assessment. Although the microbial electrode-respiration based biotransformation process could significantly detoxify some antibiotic contaminants, e.g. chloramphenicol (CAP), the response of CAP-reducing biocathode microbiome and resistome to continuous electrical stimulation, especially ARGs network interactions, are poorly understood. Here, using highthroughput functional gene array (GeoChip v4.6) and Illumina 16S rRNA gene MiSeq sequencing, the structure, composition, diversity and network interactions of CAP-reducing biocathode microbiome and resistome in response to continuous electrical stimulation were investigated. Our results indicate that the CAP bioelectroreduction process could significantly accelerate the elimination of antibacterial activity of CAP during CAP-containing wastewater treatment compared to the pure bioreduction process. Continuous electrical stimulation could obviously alter both the microbiome and resistome structures and consistently decrease the phylogenetic, functional and overall ARGs diversity and network complexity within the CAP-reducing biofilms. The relative abundances of overall ARGs and specific CAP resistance related major facilitator superfamily (MFS) transporter genes were significantly negatively correlated with the reduction efficiency of CAP to inactive antibacterial product AMCl (partially dechlorinated aromatic amine), which may reduce the ecological risk associated with the evolution of multidrug-resistant bacteria and ARGs during antibiotic-containing wastewater treatment process. This study offers new insights into the response of an antibiotic reducing biocathode resistome to continuous electrical stimulation and provides useful information on the assessment of overall ARGs risk for the bioelectrochemical treatment of antibiotic contaminants.

1. Introduction

Global-scale pollution of various environmental settings with diverse antibiotics and antibiotic resistance genes (ARGs) has attracted considerable attention (Garner et al., 2018; Li et al., 2015; Van Boeckel et al., 2015; Zhang et al., 2015; Zhu et al., 2013, 2017). The deep elimination of emerging antibiotic contaminants with high-efficiency and low-cost ways towards different water environments is one of the important goals and scientific frontiers in ensuring the global water safety (Eggen et al., 2014; Larsen et al., 2016; Pruden, 2014). The microbial-dominated biotechnology has the advantages of environmental friendliness, and low operating costs, and it is a commonly used technology all over the world (van Loosdrecht and Brdjanovic, 2014; Yun et al., 2017b). However, on one hand, traditional biological treatment systems have been confined by their low detoxification/transformation efficiency and instability for these toxic emerging contaminants (Gonzalez-Gil et al., 2016; Tran et al., 2016); on the other hand, the biological treatment method is not only referred to the degradation/

* Corresponding author. Key Laboratory of Environmental Biotechnology, Research Center for Eco-Environmental Sciences, Chinese Academy of Sciences, Beijing, 100085, China. ,
E-mail addresses: ajwang@rcees.ac.cn, waj0578@hit.edu.cn (A. Wang).

https://doi.org/10.1016/j.watres.2018.10.073
0043-1354/

attenuation process of antibiotic contaminants, but also associated with the ARGs transmission, evolution, and dynamic changes (Aydin et al., 2015; Liu et al., 2012; Varela et al., 2014). Recent findings have indicated that most ARGs could not be efficiently removed by traditional anaerobic digestion treatment (Christgen et al., 2015; Ju et al., 2016; Yang et al., 2014). As a result, wastewater treatment plants are hotspots for the release of antibiotics, and transmission of diverse antibiotic resistance bacteria (ARB) as well as ARGs into various environments (Christou et al., 2017; Czekalski et al., 2014; Guo et al., 2017a; Michael et al., 2013). Undoubtedly, activated sludge microbiome is the core element that associated with antibiotic biodegradation/biotransformation during wastewater biological treatment. Therefore, how to stimulate the anaerobic sludge microbiome and how to develop bioaugmented treatment technologies are central issues in environmental biotechnology for the enhanced treatment of high-risk antibiotic wastewater.

Bioelectrochemical systems (BES), employing electrode-respiring microbiomes to catalyze oxidative reactions in anode or reductive reactions in cathode, respectively, have attracted growing attention in recent decades (Jiang et al., 2018; Wang et al., 2011; Yun et al., 2017a, 2018). Bioelectrochemical treatment of various antibiotic contaminants including chloramphenicol (CAP), nitrofurazone, cefazolin, oxytetracycline (OTC), and sulfamethoxazole (SMX) with acclimated biocathode or bioanode microbiomes have been extensively studied. Electrical stimulation could significantly enhance these enriched electrode biofilm microbiomes for the degradation/transformation of antibiotic contaminants (Cheng et al., 2016; Kong et al., 2017; Liang et al., 2013, 2016; Wang et al., 2016; Yan et al., 2018; Zhang et al., 2017, 2018). Recent works have uncovered the specific ARGs and mobile genetic elements profile in several antibiotics (CAP, SMX, or OTC) degrading electrode microbiomes using traditional or high-throughput quantitative PCR (Guo et al., 2017b, 2018; Yan et al., 2018; Zhang et al., 2016). Guo et al. found that the higher CAP concentration, less negative cathode potential or lower salinity enhanced the expression of CAP resistance genes (e.g. *floR* and *cmlA*) and other ARGs (*intI1* and *sul1*) during the bioelectrochemical reduction (bioelectroreduction) of CAP (Guo et al., 2017b, 2018). Yan et al. found that the number of ARGs and the normalized copy number of specific tetracycline (TC) and sulfonamide resistance genes in OTC-degrading anode biofilms were both lower than those in conventional anaerobic reactors (Yan et al., 2018). In another study, the target SMX and TC associated ARGs in the biocathode were present at higher concentrations than those in the bioanode of the SMX and TC treating up-flow bioelectrochemical reactors (Zhang et al., 2016). Generally, antibiotics could trigger the cross-resistance of other antibiotic classes. For example, CAP is able to induce the cross-resistance to (fluoro) quinolones (e.g. norfloxacin and nalidixic acid), TC, β-lactams (e.g. ampicillin, cephalothin, and penicillin G), rifampicin, or vancomycin in bacteria (Cohen et al., 1989; George and Levy, 1983; Gould et al., 2004). Therefore, it is necessary to explore the changes in the diversity and abundance of other antibiotic classes resistance genes during the specific antibiotic biodegradation process. However, the response of overall resistome of the specific antibiotics-degrading electrode microbiome to continuous electrical stimulation remains poorly understood.

The objectives of this study were to determine (i) whether continuous electrical stimulation could significantly enhance the bioelectroreduction of CAP to inactive antibacterial product AMCl (partially dechlorinated aromatic amine); (ii) whether continuous electrical stimulation could obviously alter phylogenetic and functional microbiome structure, diversity and network interactions, especially the resistome profile and network interactions of CAP-reducing biofilms, and (iii) whether the enhanced CAP bioelectroreduction process could dramatically lower the diversity, abundance, and network complexity of overall ARGs. Our results suggest that the CAP bioelectroreduction process could accelerate the elimination of antibacterial activity of CAP during antibiotic-containing wastewater treatment comparing to the traditional bioreduction process, which may reduce the ecological risks of evolution of multidrug-resistant bacteria and novel ARGs. This study offers new insights into the response of an antibiotic reducing biocathode resistome to continuous electrical stimulation and provides useful information on the assessment of overall ARGs risk for the bioelectrochemical treatment of antibiotic contaminants.

2. Materials and methods

2.1. Bioelectrochemical reactors setup

The dual-chamber BES reactor was configured as described previously (Kong et al., 2015) with graphite fiber brush as both anode and cathode (2.5 cm in diameter and 2.5 cm in length) and a Ag/AgCl reference electrode (0.197 V vs. standard hydrogen electrode, SHE, Bioanalytical Systems, Inc., West Lafayette, IN, U.S.) as the reference electrode. A high-precision resistor (10 Ω) with the external power (0.5 V) in series was employed for the connection. The electrode is filled in the bioreactor, and is substantially in full contact with the catholyte (approximately 28 mL). The concentration gradient between the electrode and the catholyte is small, and mass transfer is not the main limiting factor of the reaction. The anodic and cathodic potentials were recorded every 10 min by a data acquisition system (Keithley 2700, Keithley Co. Ltd., U.S.), which were automatically converted to current according to Ohm law. All of the potential data reported herein were against SHE.

Twelve bioelectrochemical reactors were started up with 0.5 V voltage supply. Bioanode provides approximately 0.50 V voltage (vs. Ag/AgCl reference electrode, Bioanalytical Systems, Inc., West Lafayette, IN, U.S.), thus, the biocathode potential is around −0.8 V vs. SHE. The detailed bioanode establishment process was specifically described in a previous study (Wang et al., 2011). To establish the biocathode BES, the cathode chamber was filled with a mixture of the acclimated CAP-reducing consortium (by inoculating the sludge from a wastewater treatment plant, Norman, U.S.) and catholyte (0.31 g/L NH4Cl, 0.1 g/L KCl, 10 mL/L Wolf's vitamins, 10 mL/L Wolf's trace elements, 0.5 g/L glucose, 30 mg/L CAP, 50 mM phosphate buffered saline, pH = 7) at 1:3 (v/v) and incubated for 4 d with the applied voltage of 0.5 V. Subsequently, the cathode liquid content was discharged and the cathode chamber was replenished with a fresh mixture. This procedure was repeated for four times to achieve the development of biofilm on the cathode (Liang et al., 2013). Afterwards, 12 bioreactors with biocathode mode were operated for one fed batch cycle under consistent operational condition. Then 6 bioreactors continued to run under power supply mode (termed closed circuit biocathode, ^{C}biocathode), and another 6 bioreactors performed without power supply under open circuit mode (named open circuit biocathode, ^{O}biocathode). The ^{C}biocathode and ^{O}biocathode biofilms were established with the same initial inoculation and under consistent operational condition. The temperature (25 ± 1 °C) throughout the experiment was maintained in a constant temperature incubator. All the bioreactors performed 34 cycles to reach the stable state with the CAP reduction efficiency as an indicator.

2.2. GeoChip hybridization, 16S rRNA gene sequencing and data analysis

A detailed description of the DNA extraction, DNA purity and

quantity determination, PCR amplification, 16S rRNA gene Illumina MiSeq sequencing, GeoChip hybridization and data analysis were carried out according to a previous study (Liang et al., 2016). The detailed information for the used primers was described in SI (Table S1). Six ^{C}biocathode and ^{O}biocathode biofilms respectively were selected for GeoChip hybridization and 16S rRNA gene sequencing analysis. Extracted DNA (1.0 μg) from each sample was labeled with Cy-3 dye and then hybridized with GeoChip v4.6 as described previously (Tu et al., 2014). The spots with signal-to-noise ratios (SNR) lower than 2 were removed before statistical analysis. The analysis of the raw data from 16S rRNA gene sequencing was described elsewhere (Qu et al., 2015). Microbial functional gene and phylogenetic diversity indices including richness (detected functional gene or identified OTU numbers in each sample), Shannon-Weaver index (*H*) and Simpson reciprocal (*1/D*) were calculated according to a previous study (Liang et al., 2016). Detrended correspondence analysis (DCA), pearson correlation analysis, three nonparametric tests (multiple-response permutation procedure [MRPP], permutational multivariate analysis of variance [Adonis], and analysis of similarity [ANOSIM]) were calculated using R v.3.2.5. Hierarchical clustering analysis was performed using CLUSTER v3.0 and visualized by TREEVIEW (Liang et al., 2016). All functional genes detected in at least 3 out of 6 biological replicates were used for further statistical analysis. Differences between treatments were statistically analyzed by the two-tailed unpaired *t*-test.

2.3. Network construction with random matrix theory-based approach and network analysis

To elucidate microbial, functional gene, and ARG interactions in the CAP-reducing biofilm microbiomes in response to continuous electrical stimulation, two groups of phylogenetic, functional, and ARG molecular ecological networks (MENs) were constructed via random matrix theory-based interface approach in MEN analysis pipeline (MENA, http://ieg2.ou.edu/MENA/) (Deng et al., 2012; Zhou et al., 2010, 2011). The whole process was described in previous studies (Deng et al., 2012; Feng et al., 2017). Phylogenetic MENs were constructed based on the identified OTUs from 16S rRNA gene Illumina sequencing, and functional MENs were constructed based on the detected bacterial functional genes involving in antibiotic resistance, organic remediation, electron transfer and carbon-nitrogen-sulphur cycling processes from Geochip hybridization analysis. Specific ARG MENs were constructed based on the detected ARGs from Geochip hybridization analysis. Six biological replicates were used for three kinds of network analysis. Network properties including R^2 of power law, average connectivity, average path length, average clustering coefficient and modularity were all calculated in MENA pipeline (Deng et al., 2012) (Table 1). The constructed networks for the ^{C}biocathode and ^{O}biocathode biofilms were visualized using Cytoscape 3.3.0 software (Shannon et al., 2003).

2.4. Chemicals and analytical methods

CAP (>98% purity) and high-performance liquid chromatography (HPLC) grade methanol were purchased from Sigma-Aldrich (St. Louis, MO, U.S.). Other chemicals used in this study were of analytical grade.

Effluent samples taken from the cathodic chamber within 50 h were filtered through a 0.22 μm filter before chemical analysis. The concentrations of CAP, the CAP transformation products $AMCl_2$ (the nitro-group reduced product of CAP), AMCl (the partially dechlorinated product of $AMCl_2$), CAP-acetyl (acetylation of 3-hydroxyl of CAP to form CAP-acetyl) were measured using a reverse-phase HPLC system (Agilent 1200 Series, U.S.)(Liang et al., 2013). The CAP transformation products were identified by a HPLC-MS as described elsewhere (Kong et al., 2015; Liang et al., 2013). The CAP reduction efficiency (E_{rCAP}, %) was evaluated based on the difference between influent and effluent CAP concentrations.

3. Results

3.1. Biocathode reactors performance

An abiotic cathode control group is crucial for the conclusion that the biocathode group significantly enhanced the reduction of CAP. The abiotic cathode treatment results showed that CAP reduction and product AMCl formation efficiencies were both significantly lower than the biocathode treatment group (Fig. S1), which is consistent with our previous conclusions (Liang et al., 2013, 2016). Therefore, this study mainly focused on the CAP reduction efficiency, overall microbiome and antibiotic resistome characteristics of the CAP-reducing biocathode in response to continuous electrical stimulation.

After inoculating the CAP-reducing consortium for four times, cathodic biofilms were established after 400 h. During the biofilm establishment process, the cathode potential kept approximately −0.80 V with the applied cell voltage of 0.5 V. Before the disconnection of the six biocathode reactors, the E_{rCAP} and aromatic amine products (AMCl and $AMCl_2$) formation efficiency were very close in the tested 12 biocathode reactors (divided into two groups) in the first cycle (Fig. 1). No significant difference was found at any time nodes for the CAP reduction and AMCl formation (Fig. S2). Moreover, the biocathode potential of the divided two groups at the first cycle were both kept at approximately −0.80 V vs SHE (Fig. S2).

Table 1
Major topological properties of the empirical phylogenetic and functional ARG MENs of CAP-reducing biofilms upon electrical stimulation (^{C}biocathode) or not (^{O}biocathode) and their associated random networks.

Microbiome	Empirical networks							Random networks[a]		
	Similarity threshold (s_t)	Network size (n)	R^2 of power law	Average connectivity (*avgK*)	Average path length (GD)[b]	Average clustering coefficient (*avgCC*)	Modularity (Module No.)	Average path distance (GD)	Avg. clustering coefficient (*avgCC*)	Modularity (Module No.)
^{O}biocathode[d]	0.93	248	0.703	3.298	10.375[c]	0.395[c]	0.863[c] (24)	4.686 ± 0.061	0.013 ± 0.006	0.575 ± 0.009
^{C}biocathode[d]	0.90	158	0.496	3.342	7.898[c]	0.467[c]	0.838[c] (15)	4.383 ± 0.070	0.017 ± 0.008	0.554 ± 0.010
^{O}biocathode[e]	0.95	294	0.720	2.966	1.172[c]	0.643[c]	0.959[c] (89)	4.833 ± 0.099	0.012 ± 0.006	0.616 ± 0.009
^{C}biocathode[e]	0.95	209	0.639	2.402	1.109[c]	0.583[c]	0.961[c] (70)	5.704 ± 0.238	0.009 ± 0.006	0.706 ± 0.011

[a] Random networks were generated by rewiring all nodes and links corresponding to empirical networks 100 times.
[b] GD, geodesic distance.
[c] Significant difference ($P < 0.001$) between ^{O}biocathode and Cbiocathode.
[d] Phylogenetic MENs were constructed based on the identified OTUs from 16S rRNA gene Illumina sequencing.
[e] Functional ARG MENs were constructed based on the detected ARGs from Geochip hybridization analysis.

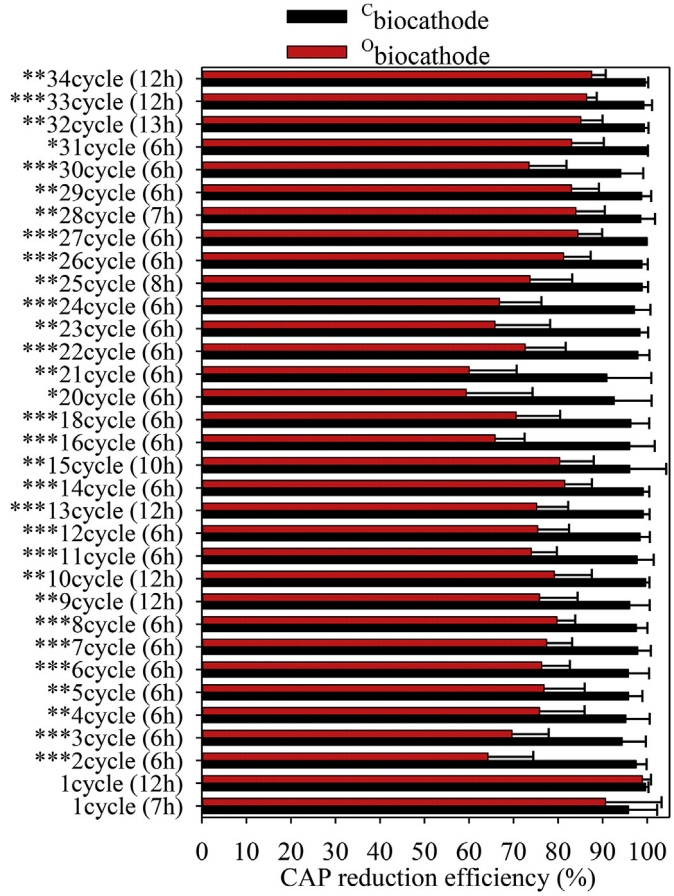

Fig. 1. Comparison of CAP reduction efficiency within 13 h between ^{C}biocathode and ^{O}biocathode. ***, ** and * denotes significance at 0.001, 0.01, and 0.05 test levels, respectively.

These results confirmed the performances consistency of the 12 biocathode reactors under same operational mode. When disconnecting the circuit of the six tested bioreactors (termed as open circuit biocathode, ^{O}biocathode), the closed circuit biocathode group (simplified as ^{C}biocathode) had a significantly higher E_{rCAP} (within 6 or 13 h) than that of the ^{O}biocathode (from the 2nd cycle to the 34th cycle) (Fig. 1). The ^{C}biocathode produced obviously more dechlorinated aromatic amine product (AMCl) from CAP reduction than that of the ^{O}biocathode within 50 h. Consistently, the ^{O}biocathode markedly accumulated the aromatic amine product ($AMCl_2$) and slightly dechlorinated $AMCl_2$ to AMCl (Fig. 2). Additionally, the ^{O}biocathode significantly accumulated more CAP-acetyl product compared with that in the ^{C}biocathode at all the operational cycles (from the 2nd to the 34th cycle) (Fig. 2), indicating the bioelectroreduction reaction could weaken the non-redox CAP acetylation resistant process. These results well indicate that the biocathodic catalysis is able to enhance the bioelectroreduction of CAP to the antibacterial inactive aromatic amine products (AMCl and $AMCl_2$).

3.2. Overall responses of the biocathode functional and phylogenetic microbiome to continuous electrical stimulation

To examine the effect of continuous electrical stimulation on the functional gene and phylogenetic diversity, structure, and composition of the biocathode microbiomes, 12 ^{C}biocathode and ^{O}biocathode biofilms (6 for each) were analyzed using high-throughput metagenomics tools microarray GeoChip (v4.6) and 16S rRNA gene Illumina MiSeq sequencing platform. DCA combined with three nonparametric dissimilarity tests (MRPP, Adonis, and ANOSIM) adequately indicated that continuous electrical stimulation significantly ($P < 0.05$) altered the functional genes and phylogenetic structure of CAP-reducing biofilms (Fig. S3 and Table S2). The overall diversity of the biocathode microbiomes was relatively lower at functional genes level and significantly lower at phylogenetic level ($P \leq 0.005$) upon continuous electrical stimulation based on the richness, *H* and *1/D* compared with those of the ^{O}biocathode microbiomes (Fig. S3), suggesting continuous electrical stimulation condition has enriched a relatively simple biocathode microbiome.

3.3. Overall responses of biocathode resistome to continuous electrical stimulation

In total, 3334 probes targeting 11 ARG families were included in GeoChip v4.6, covering 5533 coding sequences. A total of 654 ARGs were detected in 12 ^{C}biocathode and ^{O}biocathode resistomes. Hierarchical clustering analysis of these ARGs showed that 5 out of 6 ^{O}biocathode resistomes were separated from 6 ^{C}biocathode resistomes (Fig. 3a). Six ARG groups could be visualized in the heat map and 90 ARGs from groups 3 and 4 were exclusively enriched in the ^{O}biocathode. However, only 12 ARGs in group 6 were unique in the ^{C}biocathode. A total of 113 ARG genes (accounting for 17.28% of all the detected ARGs) were absolutely undetected in the ^{C}biocathode but detected at least in three ^{O}biocathode resistomes (Table S3). Meanwhile, a total of 29 ARGs (accounting for 4.43% of all the detected ARGs) were absolutely undetected in the ^{O}biocathode resistome but detected at least in 3 ^{C}biocathode resistomes (Table S4). The ^{O}biocathode enriched 3.9 times higher unique ARGs than the ^{C}biocathode. These unique ARGs from the ^{O}biocathode mainly belong to small multidrug resistance protein (SMR, 38.05%), β-lactamase (21.24%), and major facilitator superfamily efflux pump membrane fusion protein (MFS, 17.70%) categories (relative abundance >15%). The ARGs from the shared and other groups showed no significant difference between the two resistomes (Fig. 3b). In addition, 53.42% and 29.19% of the shared ARGs (amount to 161 ARGs) belong to the transporter and β-lactamase subcategories respectively. DCA also showed the significant structure difference between the ^{C}biocathode and ^{O}biocathode resistomes (Fig. 3c).

Three nonparametric dissimilarity tests (MRPP, Adonis, and ANOSIM) based on the two indices of Jaccard and Bray-Curtis together also indicated that the continuous electrical stimulation dramatically altered the CAP-reducing biocathode resistome structure ($P \leq 0.005$) (Table S2). The overall ARGs diversity of the ^{C}biocathode resistomes was marginally lowered upon the continuous electrical stimulation based on the richness, *H* and *1/D* indices ($P < 0.10$) compared to those of the ^{O}biocathode resistomes (Fig. 3d). This indicates that the persistent electrons donor of electrode could shape a relatively simple biocathode resistome.

3.4. Differences of ARGs abundance at different families

The ^{C}biocathode showed lower gene abundance of the total antibiotic resistance ($P = 0.094$), SMR ($P = 0.061$) and MFS ($P = 0.048$) than those of the ^{O}biocathode (Fig. 4). A total of 122 MFS genes (accounting for 2.20% of all the detected functional genes) were detected in this study. Twenty MFS genes were absolutely undetected in 6 ^{C}biocathode resistomes (accounting for 16.39%) but detected at least in 3 ^{O}biocathode resistomes. Comparatively, only 4 MFS genes (accounting for 3.28%) were absolutely undetected in 6 ^{O}biocathode resistomes but appeared at least in 3 ^{C}biocathode resistomes. Other ARG categories were also showed relatively lower abundance in the ^{C}biocathode than those in the ^{O}biocathode

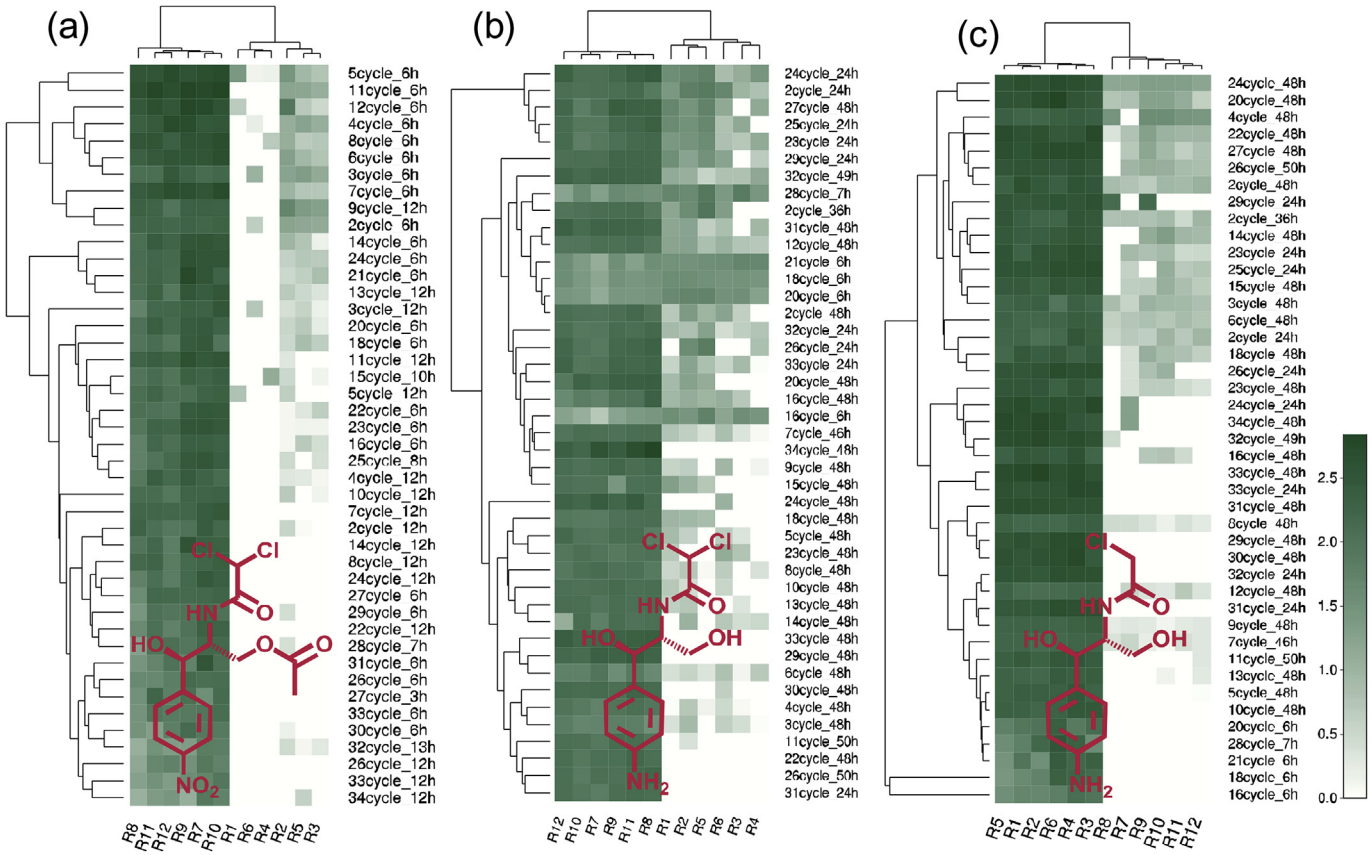

Fig. 2. Hierarchical clustering analysis of the CAP transformation products including CAP-acetyl (a), $AMCl_2$ (b) and AMCl (c) from under two operational modes (^{C}bioocathode: R1-6; ^{O}bioocathode: R7-12). The HPLC peak area of three formed products were logarithmically transformed for the hierarchical cluster analysis. Brighter green coloring indicates higher product concentration while white indicates the absence of product accumulation as shown in the color bar. (For interpretation of the references to color in this figure legend, the reader is referred to the Web version of this article.)

(Fig. 4). Pearson correlation analysis was used to explore whether the enhanced CAP bioelectroreduction process could potentially minimize the enrichment of ARGs in the biofilm microbiomes. The results showed that total abundances of all detected ARGs ($r = -0.51$, $P = 0.087$), SMR genes ($r = -0.56$, $P = 0.058$), MFS genes ($r = -0.59$, $P = 0.042$), and ABC transporter genes ($r = -0.50$, $P = 0.096$) were negatively correlated with AMCl yield, while SMR genes ($r = -0.49$, $P = 0.101$), MFS genes ($r = -0.592$, $P = 0.087$), and ABC genes ($r = -0.51$, $P = 0.094$) were also negatively correlated with CAP reduction efficiency (Fig. 5).

3.5. Effects of electrical stimulation on the overall network structure and interactions

To understand the effect of electrical stimulation on the biofilm network interactions from phylogenetic and functional genes perspectives, phylogenetic and functional MENs were constructed based on the identified 1566 OTUs from 16S rRNA gene sequencing and 15636 functional genes detected from Geochip hybridization analysis respectively. The major topological properties of phylogenetic and functional networks were summarized (Table 1 and Fig. S5). Based on the network size (the number of OTUs or genes in a network, namely node number) and total link number, the overall network complexity at phylogenetic and functional genes levels were both significantly higher under pure anaerobic condition (^{O}biocathode) than under electrical stimulation condition (^{C}biocathode). Specifically, compared to the ^{O}biocathode, the phylogenetic MENs of the ^{C}biocathode generally had significantly shorter path lengths, higher clustering efficiencies, and less modules (Table 1), which are key network properties in terms of system efficiency and robustness (Zhou et al., 2010, 2011). To better understand the interactions among different phyla and gene categories, the two networks were visualized (Figs. S4 and S5). Taken the phylogenetic MENs for example, the impact of continuous electrical stimulation on the biofilm network structure and composition could be seen from phylum level. The majority of the nodes in these two networks belonged to 11 phyla (Fig. S4). Among them, Proteobacteria, Firmicutes, Bacteroidetes, and Euryarchaeota were more dominant. Under electrical stimulation, the relative proportions of Firmicutes and Euryarchaeota in the network enriched considerably, while the percentage of Proteobacteria decreased substantially (Fig. S4). These results strongly suggest that continuous electrical stimulation could obviously affect the overall architecture of the MENs in the CAP-reducing biofilms and consistently decrease the overall network complexity.

3.6. Effects of electrical stimulation on the resistome network structure and interactions

To understand the ARG interactions within the ^{C}biocathode and ^{O}biocathode resistomes, ARG MENs were constructed based on the detected 654 ARGs from Geochip hybridization analysis. The ^{C}biocathode and ^{O}biocathode resistomes were analyzed, and the major topological properties of ARG networks were summarized (Table 1). The overall topology indices showed that the network connectivity distributions fitted with the power-law model (R^2 of

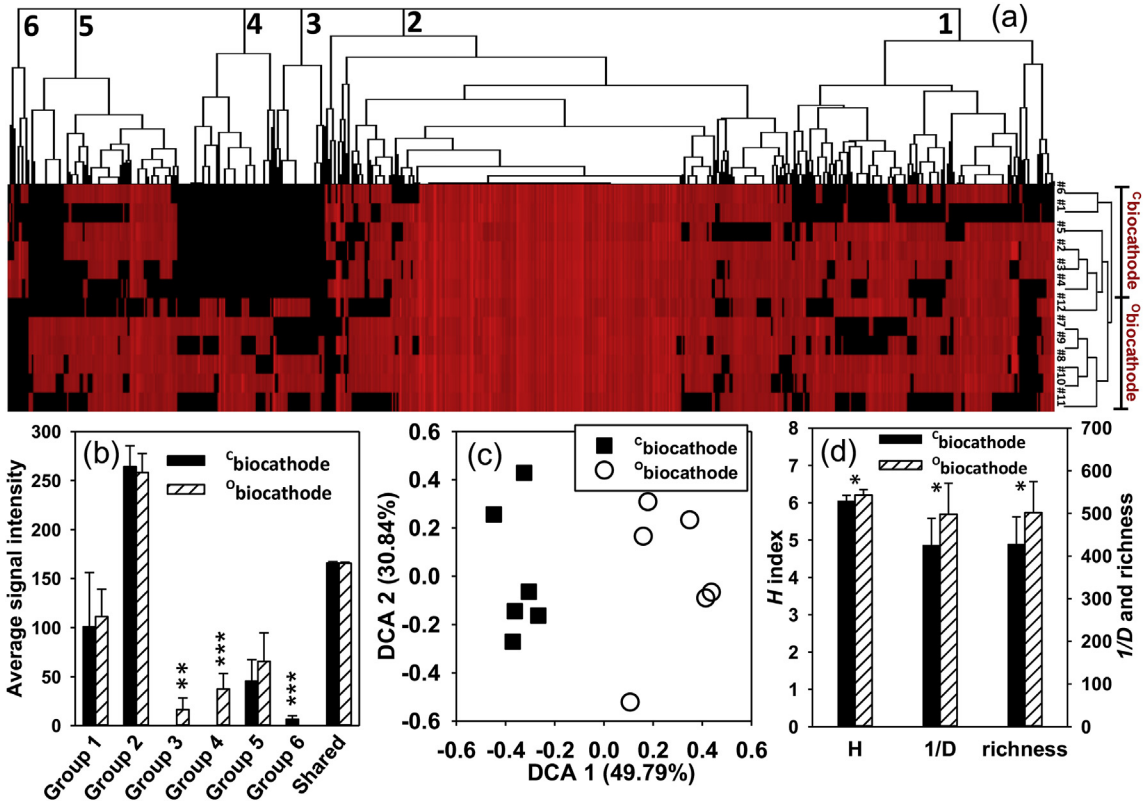

Fig. 3. Hierarchical clustering analysis of ARGs detected by GeoChip hybridization (a). The figure was generated using CLUSTER and visualized with TREEVIEW. Black represents no hybridization above background level and red represents positive hybridization. The color intensity indicates differences in signal intensity. Six different gene patterns were observed and indicated by numbers in the tree (a), and average signal intensities of these groups and shared ARGs for the ^{C}bioocathode and ^{O}bioocathode are shown (b). DCA results showing that continuous electrical stimulation markedly altered the CAP-reducing biocathode resistome structure (c). The richness (gene #), Shannon-Weaver (*H*) and invsimpson (*1/D*) indices in the ^{C}bioocathode and ^{O}bioocathode at ARG level (d). ***, ** and * denotes significance at 0.01, 0.05, and 0.10 test levels, respectively. (For interpretation of the references to color in this figure legend, the reader is referred to the Web version of this article.)

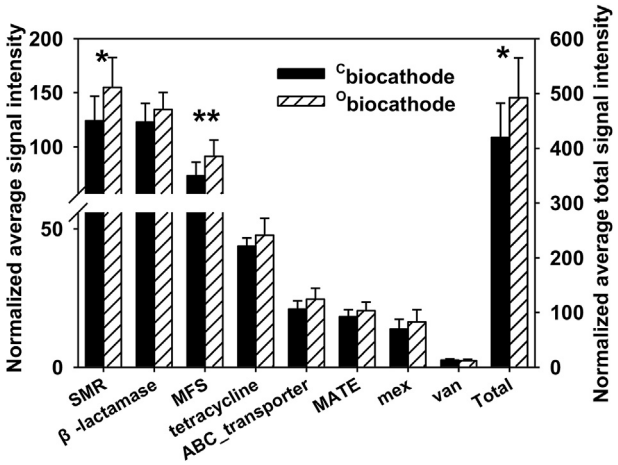

Fig. 4. The normalized signal intensity of detected ARGs of ^{C}bioocathode and ^{O}bioocathode. ABC_transporter: a ATP-binding cassette multidrug transport protein; SMR: a small multidrug resistance protein; MFS: a major facilitator superfamily efflux pump membrane fusion protein, which works as drug-efflux pumps to confer antibiotic resistance; MATE: a subfamily of the multidrug and toxic compound extrusion (MATE)-like proteins, also a multidrug resistance protein; mex is a resistance-nodulation-cell division (RND) multidrug efflux transporter; van: a putative vancomycin/teicoplanin A-type resistance protein, termed D-alanyl-D-alanine ligase. β-lactamase includes classes A, B, C and D.

power law from 0.639 to 0.720). To better understand the interactions among different ARG families, the two networks were visualized. The majority of the nodes in these two networks belonged to 4 ARG groups (MFS, β-lactamase, SMR, and Tet). The impact of continuous electrical stimulation on the biofilm resistome network structure could be seen from the ARG family level. Among them, SMR and β-lactamase genes showed more node number and proportion both in the ^{C}biocathode and ^{O}biocathode, followed by MFS and Tet (Fig. 6 and Fig. S6). Based on the node number, the network complexity for all ARG families was generally higher under pure anaerobic condition (^{O}biocathode) than under electrical stimulation condition (^{C}biocathode). Although the relative proportions of most ARG families were not obviously different between the ^{C}biocathode and ^{O}biocathode (Fig. S5), the ^{O}biocathode resistome had a more complex and quite different network structure than the ^{C}biocathode resistome, based on the average connectivity (*avgK*, from 2.402 to 2.966), node numbers (from 209 to 294) and link numbers (from 633 to 957) (Table 1). Specifically, the ^{O}biocathode resistome had significantly more total positive (691 vs 473) and negative (266 vs 160) links than those of the ^{C}biocathode resistome (Fig. S6). More positive correlations imply the co-existence of diverse ARGs during the bioreduction of CAP. For modules property, a total of 14 modules with ≥5 nodes were obtained for the ^{O}biocathode networks, while the ^{C}biocathode networks had 4 modules with >5 nodes (Fig. 6).

We also further analyzed the MFS genes networks property because CAP resistance genes mainly belong to this family and it showed obviously lower gene abundances in the ^{C}biocathode than that of the ^{O}biocathode ($P < 0.05$). The number of MFS nodes and total links in the networks obviously decreased 1.90 and 2.18 times

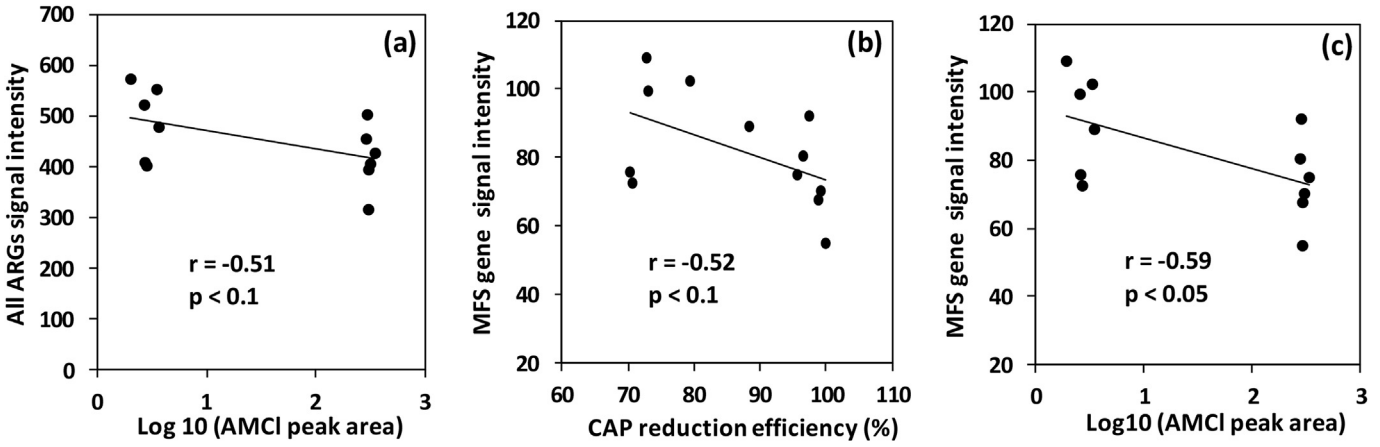

Fig. 5. Correlations between CAP reduction/AMCl formation efficiencies and the average signal intensity of all ARGs/specific MFS genes. Scatterplots of CAP reduction data vs intensity of all ARGs/specific MFS genes are shown along with linear regression lines.

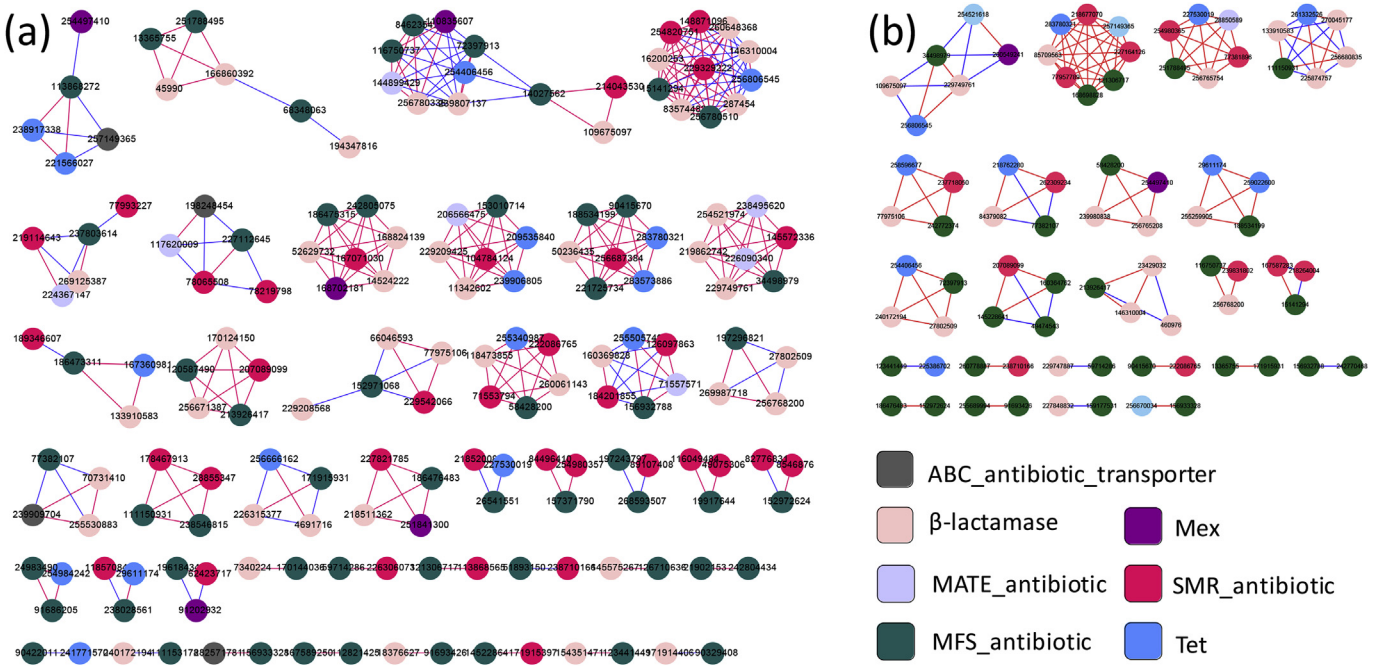

Fig. 6. Networks to visualize interactions among the detected ARGs from seven ARG families in the ^{O}biocathode (a) and ^{C}biocathode (b) resistomes. Blue lines stand for negative interactions between nodes and pink lines stand for positive interactions. (For interpretation of the references to color in this figure legend, the reader is referred to the Web version of this article.)

respectively upon continuous electrical stimulation. Moreover, whether it is the ^{C}biocathode or the ^{O}biocathode, the proportion of positive links is greater (>70%). Collectively, the ARG networks had considerably smaller network size, significantly lower connectivity, shorter path lengths, and lower clustering efficiencies under continuous electrical stimulation than under no electrical stimulation. Consistent to the phylogenetic and functional MENs, continuous electrical stimulation also obviously altered the resistome network structure and impacted the network interactions among various ARG families and markedly decreased the resistome network complexity in the anaerobic CAP-reducing biofilm system.

4. Discussion

Understanding the fate and profile of overall resistome during the biological treatment of antibiotic-containing wastewater is a central issue for the water ecological safety assessment. Recent studies largely focused on the fate of the selected antibiotic-associated ARGs but not overall ARGs during the bio-electrochemical treatment of different antibiotic contaminants (Guo et al., 2017b, 2018; Yan et al., 2018; Zhang et al., 2016). Concretely, Zhang et al. found that the target SMX and TC ARGs (*sulI*, *sulII*, *sulIII*, *tetA*, *tetC*, *tetO*, *tetQ*, and *tetW*) in the lower biocathode were present at a higher concentration than in the upper bioanode of the SMX and TC treating up-flow BESs, which is consistent with the bioanode zone showed the higher antibiotic removal efficiency than that of the biocathode zone (Zhang et al., 2016). Guo et al. investigated the fate of ARGs such as CAP (*floR* and *cmlA*), SMX (*sulI*) and TC (*tetC*) resistance as well as mobile genetic element integrase (*intI1*) encoding genes during the

bioelectroreduction of CAP in the biocathode under different operational modes. A higher CAP concentration (20 mg/L and 50 mg/L compared to 10 mg/L) and less negative cathode potential (−0.5 V vs SHE, with the lowest CAP reduction efficiency compared to that of the −1.25 V and −1.0 V operational modes) enhanced the expression of CAP resistance genes (e.g., *floR* and *cmlA*) (Guo et al., 2017b). These results suggest that the enhanced antibiotic reduction could reduce the relative abundances of the specific ARGs in the functional electrode-respiring biofilms (Guo et al., 2017b; Yan et al., 2018; Zhang et al., 2016), which also agreed with that high antibiotic residual generally could increase the ARGs abundance within anaerobic bioreactors (Guo et al., 2017c). Interestingly, Guo et al. also uncovered the distinct responses of representative ARGs abundance of CAP-reducing biocathode to salinity gradient. The relative abundances of *cmlA*, *floR*, *intI1* and *sul1* under low salinity group (0.5%) were significantly higher than those of the control and high salinity group (2% and 6%), although the control (88.3%) and high 6% salinity group (49.5%) showed lower CAP reduction efficiency than that of the low 0.5% salinity group (92.5%). Differently, the relative abundance of *tetC* significantly increased as salinity increased (Guo et al., 2018). However, the response of overall resistome of the involved electrode-associated multispecies biofilms, especially the network structure and interactions to continuous electrical stimulation has not yet been reported.

Using a comprehensive functional gene microarray GeoChip, which contains 3334 probes targeting 11 ARG families, this study examined the CAP-reducing cathode biofilm resistomes under continuous electrical stimulation, and analyzed the overall ARGs structure, composition, diversity, abundance, and network interactions of the biocathode microbiomes with the pure anaerobic biofilm microbiomes as the control to understand how the biofilm resistome respond to continuous electrical stimulation during CAP reduction. The results showed that the overall ^{C}biocathode and ^{O}biocathode resistome structures were significantly different and the relative abundances of various ARG families, especially MFS transporter genes, which cover CAP resistance genes (e.g. *floR*, *cmlA*, *fexA*, *fexB* and *pexA*) (Li et al., 2013), were obviously lower in the ^{C}biocathode than those in the ^{O}biocathode. Moreover, the relative abundance of MFS genes was marginally or significantly negatively correlated with CAP reduction efficiency ($r = -0.592$, $P = 0.087$) and AMCl yield ($r = -0.59$, $P = 0.042$). In addition, the CAP bioelectroreduction reaction can also weaken the non-redox CAP acetylation resistant process based on the chemical data (Fig. 2a). The enhanced bioelectroreduction of CAP to AMCl appeared to exert smaller antibiotic selection pressure on the ^{C}biocathode microbiomes, and finally resulted in a significantly lower total ARGs abundance, especially for specific CAP-associated MFS genes. More importantly, continuous electrical stimulation could consistently decrease the phylogenetic, functional and overall ARGs diversity and network complexity within the CAP-reducing biofilms. These results highlight that continuous electrical stimulation could minimize the possibility of evolution of multidrug-resistant bacteria and novel ARGs by accelerating antibiotic detoxification during antibiotics-containing wastewater treatment. This information may be useful for the assessment of overall ARGs risk for the bioelectrochemical treatment of antibiotic contaminants.

5. Conclusions

The CAP bioelectroreduction process can significantly accelerate the elimination of antibacterial activity of CAP during antibiotic-containing wastewater treatment compared to the pure bioreduction process. Continuous electrical stimulation obviously altered the resistome structure and decreased the ARGs diversity, abundance and network complexity within the CAP-reducing biocathode microbiomes. The relative abundance of CAP resistance associated MFS transporter genes was significantly negatively correlated with the reduction efficiency of CAP to AMCl. These results strongly suggest that such a process has its advantage over conventional anaerobic treatment process on the minimization of the evolution of multidrug-resistant bacteria and ARGs by accelerating antibiotic detoxification during antibiotic-containing wastewater treatment. This study offers new insights into the response of an antibiotics reducing biocathode resistome to continuous electrical stimulation and provides potentially useful information for the assessment of overall ARGs risk for the bioelectrochemical treatment of antibiotic contaminants.

Acknowledgments

This work was supported by the National Natural Science Foundation of China (No. 31870102 and 31500084), and the Key Research Program of the Chinese Academy of Sciences (No. KFZD-SW-219).

Appendix A. Supplementary data

Supplementary data to this article can be found online at https://doi.org/10.1016/j.watres.2018.10.073.

References

Aydin, S., Ince, B., Ince, O., 2015. Development of antibiotic resistance genes in microbial communities during long-term operation of anaerobic reactors in the treatment of pharmaceutical wastewater. Water Res. 83, 337–344.
Cheng, Z., Hu, X., Sun, Z.R., 2016. Microbial community distribution and dominant bacterial species analysis in the bio-electrochemical system treating low concentration cefuroxime. Chem. Eng. J. 303, 137–144.
Christgen, B., Yang, Y., Ahammad, S.Z., Li, B., Rodriquez, D.C., Zhang, T., Graham, D.W., 2015. Metagenomics shows that low-energy anaerobic-aerobic treatment reactors reduce antibiotic resistance gene levels from domestic wastewater. Environ. Sci. Technol. 49 (4), 2577–2584.
Christou, A., Aguera, A., Bayona, J.M., Cytryn, E., Fotopoulos, V., Lambropoulou, D., Manaia, C.M., Michael, C., Revitt, M., Schroder, P., Fatta-Kassinos, D., 2017. The potential implications of reclaimed wastewater reuse for irrigation on the agricultural environment: the knowns and unknowns of the fate of antibiotics and antibiotic resistant bacteria and resistance genes - a review. Water Res. 123, 448–467.
Cohen, S.P., Mcmurry, L.M., Hooper, D.C., Wolfson, J.S., Levy, S.B., 1989. Cross-resistance to fluoroquinolones in multiple-antibiotic-resistant (mar) escherichia-coli selected by tetracycline or chloramphenicol - decreased drug accumulation associated with membrane-changes in addition to ompf reduction. Antimicrob. Agents Chemother. 33 (8), 1318–1325.
Czekalski, N., Diez, E.G., Burgmann, H., 2014. Wastewater as a point source of antibiotic-resistance genes in the sediment of a freshwater lake. ISME J. 8 (7), 1381–1390.
Deng, Y., Jiang, Y.H., Yang, Y., He, Z., Luo, F., Zhou, J., 2012. Molecular ecological network analyses. BMC Bioinf. 13, 113.
Eggen, R.I.L., Hollender, J., Joss, A., Scharer, M., Stamm, C., 2014. Reducing the discharge of micropollutants in the aquatic environment: the benefits of upgrading wastewater treatment plants. Environ. Sci. Technol. 48 (14), 7683–7689.
Feng, K., Zhang, Z., Cai, W., Liu, W., Xu, M., Yin, H., Wang, A., He, Z., Deng, Y., 2017. Biodiversity and species competition regulate the resilience of microbial biofilm community. Mol. Ecol. 26 (21), 6170–6182.
Garner, E., Chen, C., Xia, K., Bowers, J., Engelthaler, D.M., McLain, J., Edwards, M.A., Pruden, A., 2018. Metagenomic characterization of antibiotic resistance genes in full-scale reclaimed water distribution systems and corresponding potable systems. Environ. Sci. Technol. 52 (11), 6113–6125.
George, A.M., Levy, S.B., 1983. Amplifiable resistance to tetracycline, chloramphenicol, and other antibiotics in Escherichia coli: involvement of a non-plasmid-determined efflux of tetracycline. J. Bacteriol. 155 (2), 531–540.
Gonzalez-Gil, L., Papa, M., Feretti, D., Ceretti, E., Mazzoleni, G., Steimberg, N., Pedrazzani, R., Bertanza, G., Lema, J.M., Carballa, M., 2016. Is anaerobic digestion effective for the removal of organic micropollutants and biological activities from sewage sludge? Water Res. 102, 211–220.
Gould, C.V., Fishman, N.O., Nachamkin, I., Lautenbach, E., 2004. Chloramphenicol resistance in vancomycin-resistant enterococcal bacteremia: impact of priop fluoroquinolone use? Infect. Control Hosp. Epidemiol. 25 (2), 138–145.
Guo, J.H., Li, J., Chen, H., Bond, P.L., Yuan, Z.G., 2017a. Metagenomic analysis reveals wastewater treatment plants as hotspots of antibiotic resistance genes and

mobile genetic elements. Water Res. 123, 468–478.
Guo, N., Wang, Y.K., Tong, T.Z., Wang, S.G., 2018. The fate of antibiotic resistance genes and their potential hosts during bio-electrochemical treatment of high-salinity pharmaceutical wastewater. Water Res. 133, 79–86.
Guo, N., Wang, Y.K., Yan, L., Wang, X.H., Wang, M.Y., Xu, H., Wang, S.G., 2017b. Effect of bio-electrochemical system on the fate and proliferation of chloramphenicol resistance genes during the treatment of chloramphenicol wastewater. Water Res. 117, 95–101.
Guo, X.P., Pang, W.H., Dou, C.L., Yin, D.Q., 2017c. Sulfamethoxazole and COD increase abundance of sulfonamide resistance genes and change bacterial community structures within sequencing batch reactors. Chemosphere 175, 21–27.
Jiang, X.B., Shen, J.Y., Xu, K.C., Chen, D., Mu, Y., Sun, X.Y., Han, W.Q., Li, J.S., Wang, L.J., 2018. Substantial enhancement of anaerobic pyridine bio-mineralization by electrical stimulation. Water Res. 130, 291–299.
Ju, F., Li, B., Ma, L.P., Wang, Y.B., Huang, D.P., Zhang, T., 2016. Antibiotic resistance genes and human bacterial pathogens: Co-occurrence, removal, and enrichment in municipal sewage sludge digesters. Water Res. 91, 1–10.
Kong, D., Liang, B., Yun, H., Cheng, H., Ma, J., Cui, M., Wang, A., Ren, N., 2015. Cathodic degradation of antibiotics: characterization and pathway analysis. Water Res. 72, 281–292.
Kong, D.Y., Yun, H., Cui, D., Qi, M.Y., Shao, C.Y., Cui, D.C., Ren, N.Q., Liang, B., Wang, A.J., 2017. Response of antimicrobial nitrofurazone-degrading biocathode communities to different cathode potentials. Bioresour. Technol. 241, 951–958.
Larsen, T.A., Hoffmann, S., Luthi, C., Truffer, B., Maurer, M., 2016. Emerging solutions to the water challenges of an urbanizing world. Science 352 (6288), 928–933.
Li, B., Yang, Y., Ma, L.P., Ju, F., Guo, F., Tiedje, J.M., Zhang, T., 2015. Metagenomic and network analysis reveal wide distribution and co-occurrence of environmental antibiotic resistance genes. ISME J. 9 (11), 2490–2502.
Li, J., Shao, B., Shen, J.Z., Wang, S.C., Wu, Y.N., 2013. Occurrence of chloramphenicol-resistance genes as environmental pollutants from swine feedlots. Environ. Sci. Technol. 47 (6), 2892–2897.
Liang, B., Cheng, H.Y., Kong, D.Y., Gao, S.H., Sun, F., Cui, D., Kong, F.Y., Zhou, A.J., Liu, W.Z., Ren, N.Q., Wu, W.M., Wang, A.J., Lee, D.J., 2013. Accelerated reduction of chlorinated nitroaromatic antibiotic chloramphenicol by biocathode. Environ. Sci. Technol. 47 (10), 5353–5361.
Liang, B., Kong, D., Ma, J., Wen, C., Yuan, T., Lee, D.J., Zhou, J., Wang, A., 2016. Low temperature acclimation with electrical stimulation enhance the biocathode functioning stability for antibiotics detoxification. Water Res. 100, 157–168.
Liu, M.M., Zhang, Y., Yang, M., Tian, Z., Ren, L.R., Zhang, S.J., 2012. Abundance and distribution of tetracycline resistance genes and mobile elements in an oxytetracycline production wastewater treatment system. Environ. Sci. Technol. 46 (14), 7551–7557.
Michael, I., Rizzo, L., McArdell, C.S., Manaia, C.M., Merlin, C., Schwartz, T., Dagot, C., Fatta-Kassinos, D., 2013. Urban wastewater treatment plants as hotspots for the release of antibiotics in the environment: a review. Water Res. 47 (3), 957–995.
Pruden, A., 2014. Balancing water sustainability and public health goals in the face of growing concerns about antibiotic resistance. Environ. Sci. Technol. 48 (1), 5–14.
Qu, Y.Y., Ma, Q., Deng, J., Shen, W.L., Zhang, X.W., He, Z.L., Van Nostrand, J.D., Zhou, J.T., Zhou, J.Z., 2015. Responses of microbial communities to single-walled carbon nanotubes in phenol wastewater treatment systems. Environ. Sci. Technol. 49 (7), 4627–4635.
Shannon, P., Markiel, A., Ozier, O., Baliga, N.S., Wang, J.T., Ramage, D., Amin, N., Schwikowski, B., Ideker, T., 2003. Cytoscape: a software environment for integrated models of biomolecular interaction networks. Genome Res. 13 (11), 2498–2504.
Tran, N.H., Chen, H., Reinhard, M., Mao, F., Gin, K.Y., 2016. Occurrence and removal of multiple classes of antibiotics and antimicrobial agents in biological wastewater treatment processes. Water Res. 104, 461–472.
Tu, Q., Yu, H., He, Z., Deng, Y., Wu, L., Van Nostrand, J.D., Zhou, A., Voordeckers, J., Lee, Y.J., Qin, Y., Hemme, C.L., Shi, Z., Xue, K., Yuan, T., Wang, A., Zhou, J., 2014. GeoChip 4: a functional gene-array-based high-throughput environmental technology for microbial community analysis. Mol. Ecol. Resour. 14 (5), 914–928.
Van Boeckel, T.P., Brower, C., Gilbert, M., Grenfell, B.T., Levin, S.A., Robinson, T.P., Teillant, A., Laxminarayan, R., 2015. Global trends in antimicrobial use in food animals. Proc. Natl. Acad. Sci. U. S. A 112 (18), 5649–5654.
van Loosdrecht, M.C., Brdjanovic, D., 2014. Water treatment. Anticipating the next century of wastewater treatment. Science 344 (6191), 1452–1453.
Varela, A.R., Andre, S., Nunes, O.C., Manaia, C.M., 2014. Insights into the relationship between antimicrobial residues and bacterial populations in a hospital-urban wastewater treatment plant system. Water Res. 54, 327–336.
Wang, A.J., Cheng, H.Y., Liang, B., Ren, N.Q., Cui, D., Lin, N., Kim, B.H., Rabaey, K., 2011. Efficient reduction of nitrobenzene to aniline with a biocatalyzed cathode. Environ. Sci. Technol. 45 (23), 10186–10193.
Wang, L., Liu, Y.L., Ma, J., Zhao, F., 2016. Rapid degradation of sulphamethoxazole and the further transformation of 3-amino-5-methylisoxazole in a microbial fuel cell. Water Res. 88, 322–328.
Yan, W., Guo, Y., Xiao, Y., Wang, S., Ding, R., Jiang, J., Gang, H., Wang, H., Yang, J., Zhao, F., 2018. The changes of bacterial communities and antibiotic resistance genes in microbial fuel cells during long-term oxytetracycline processing. Water Res. 142, 105–114.
Yang, Y., Li, B., Zou, S.C., Fang, H.H.P., Zhang, T., 2014. Fate of antibiotic resistance genes in sewage treatment plant revealed by metagenomic approach. Water Res. 62, 97–106.
Yun, H., Liang, B., Kong, D.Y., Cheng, H.Y., Li, Z.L., Gu, Y.B., Yin, H.Q., Wang, A.J., 2017a. Polarity inversion of bioanode for biocathodic reduction of aromatic pollutants. J. Hazard Mater. 331, 280–288.
Yun, H., Liang, B., Kong, D.Y., Wang, A.J., 2018. Improving biocathode community multifunctionality by polarity inversion for simultaneous bioelectroreduction processes in domestic wastewater. Chemosphere 194, 553–561.
Yun, H., Liang, B., Qiu, J.G., Zhang, L., Zhao, Y.K., Jiang, J.D., Wang, A.J., 2017b. Functional characterization of a novel amidase involved in biotransformation of triclocarban and its dehalogenated congeners in *Ochrobactrum* sp. TCC-2. Environ. Sci. Technol. 51 (1), 291–300.
Zhang, E.R., Yu, Q.L., Zhai, W.J., Wang, F., Scott, K., 2018. High tolerance of and removal of cefazolin sodium in single-chamber microbial fuel cells operation. Bioresour. Technol. 249, 76–81.
Zhang, Q.H., Zhang, Y.Y., Li, D.P., 2017. Cometabolic degradation of chloramphenicol via a meta-cleavage pathway in a microbial fuel cell and its microbial community. Bioresour. Technol. 229, 104–110.
Zhang, Q.Q., Ying, G.G., Pan, C.G., Liu, Y.S., Zhao, J.L., 2015. Comprehensive evaluation of antibiotics emission and fate in the river basins of China: source analysis, multimedia modeling, and linkage to bacterial resistance. Environ. Sci. Technol. 49 (11), 6772–6782.
Zhang, S., Song, H.L., Yang, X.L., Yang, K.Y., Wang, X.Y., 2016. Effect of electrical stimulation on the fate of sulfamethoxazole and tetracycline with their corresponding resistance genes in three-dimensional biofilm-electrode reactors. Chemosphere 164, 113–119.
Zhou, J., Deng, Y., Luo, F., He, Z., Tu, Q., Zhi, X., 2010. Functional molecular ecological networks. mBio 1 (4). https://doi.org/10.1128/mBio.00169-10 e00169-10.
Zhou, J., Deng, Y., Luo, F., He, Z., Yang, Y., 2011. Phylogenetic molecular ecological network of soil microbial communities in response to elevated CO_2. mBio 2 (4). https://doi.org/10.1128/mBio.00122-11 e00122-11.
Zhu, Y.G., Johnson, T.A., Su, J.Q., Qiao, M., Guo, G.X., Stedtfeld, R.D., Hashsham, S.A., Tiedje, J.M., 2013. Diverse and abundant antibiotic resistance genes in Chinese swine farms. Proc. Natl. Acad. Sci. U. S. A 110 (9), 3435–3440.
Zhu, Y.G., Zhao, Y., Li, B., Huang, C.L., Zhang, S.Y., Yu, S., Chen, Y.S., Zhang, T., Gillings, M.R., Su, J.Q., 2017. Continental-scale pollution of estuaries with antibiotic resistance genes. Nat. Microbiol. 2 (4), 16270.